Hindawi Publishing Corporation
Journal of Nanomaterials
Volume 2014, Article ID 183954, 6 pages
http://dx.doi.org/10.1155/2014/183954

Research Article

Room Temperature Optical Constants and Band Gap Evolution of Phase Pure M_1-VO_2 Thin Films Deposited at Different Oxygen Partial Pressures by Reactive Magnetron Sputtering

Meng Jiang,[1,2] Yamei Li,[1,2] Shaotang Li,[1,2] Huaijuan Zhou,[1,2] Xun Cao,[1] Shanhu Bao,[1] Yanfeng Gao,[1,3] Hongjie Luo,[1,3] and Ping Jin[1]

[1] *State Key Laboratory of High Performance Ceramics and Superfine Microstructure, Shanghai Institute of Ceramics (SIC), Chinese Academy of Sciences (CAS), Dingxi 1295, Changning, Shanghai 200050, China*
[2] *Graduate University of Chinese Academy of Sciences, Yuquanlu 19, Beijing 100049, China*
[3] *School of Materials Science and Engineering, Shanghai University, 99 Shangda, Shanghai 200444, China*

Correspondence should be addressed to Ping Jin; p-jin@mail.sic.ac.cn

Received 13 October 2013; Accepted 11 December 2013; Published 2 January 2014

Academic Editor: Yoshitake Masuda

Spectroscopic ellipsometry study was employed for phase pure $VO_2(M_1)$ thin films grown at different oxygen partial pressures by reactive magnetron sputtering. The optical constants of the $VO_2(M_1)$ thin films have been determined in a photon energy range between 0.73 and 5.05 eV. The near-infrared extinction coefficient and optical conductivity of $VO_2(M_1)$ thin films rapidly increase with decreasing O_2-Ar ratios. Moreover, two electronic transitions can be uniquely assigned. The energy gaps correlated with absorption edge (E_1) at varied O_2-Ar ratios are almost the same (~2.0 eV); consequently, the absorption edge is not significantly changed. However, the optical band gap corresponding to semiconductor-to-metal phase transition (E_2) decreases from 0.53 to 0.18 eV with decreasing O_2-Ar ratios.

1. Introduction

Vanadium dioxide (VO_2), one of the most interesting transition metal oxides, exhibits a reversible first-order semiconductor-to-metal phase transition (SMT) at a critical temperature T_c = 68°C (for bulk single crystal VO_2) [1]. VO_2 has a tetragonal rutile structure with the $P4_2/mnm$ space group (R phase) above the phase transition temperature, where the partially filled $d_{//}$ band localized at the Fermi level and the rutile phase is metallic [2]. Below the phase transition temperature, it transforms to a monoclinic structure with the $P2_1/c$ space group (M_1 phase), in which the partially filled $d_{//}$ band splits into an unoccupied part being pushed past the π^* band and a filled part with the $d_{//}$ band dropping below the Fermi level, thus opening up a bandgap of ~0.6 eV between π^* and the filled part of $d_{//}$ band [2]. Dramatic changes in the electrical and optical properties across the SMT make VO_2 thin films suitable for many applications, such as switching devices, sensors, and smart windows [3–6].

It has been noted that oxygen partial pressure has effects on the structural and resistivity transition behaviors of VO_2 [7]. Although the optimized oxygen partial pressure to fabricate VO_2 films on glass and the optical properties of those samples were investigated [8], the optical constants, especially extinction coefficient k, which is crucial in understanding band structures, are not involved. Moreover, two energy gaps E_1 and E_2 are not distinguished as well.

Low visible transparency and unfavorable yellowish colour, which are correlated with absorption edges, limit the application of VO_2 smart windows. For most practical applications the phase transition temperature T_c needs to be in the vicinity of room temperature (~25°C) and the T_c may be assumed to be correlated with the optical band gap E_2. Consequently, the distinguishment of E_1 and E_2 plays an important role in improving the performance of VO_2.

In this research, we thoroughly investigated the effects of oxygen partial pressures on the optical constants and

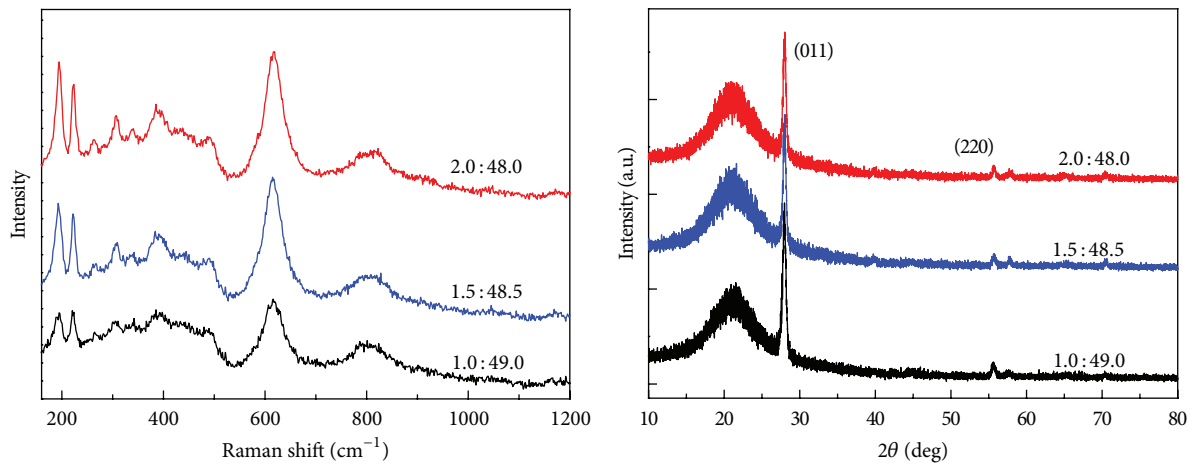

FIGURE 1: Raman (a) and XRD (b) spectra for VO_2 films deposited at different O_2-Ar ratios.

the electronic transition behaviors of phase pure $VO_2(M_1)$ thin films deposited on quartz glass by reactive magnetron sputtering. Moreover, two electronic transitions related to absorption edge (E_1) and SMT (E_2) were distinguished.

2. Experimental Section

VO_2 thin films with a thickness of ~70 nm were deposited using a reactive rf magnetron sputtering system with a water-cooled vanadium metal target (50 mm in diameter, 99.9% purity). Quartz glasses (20 × 20 × 1 mm) were used as substrates and they were ultrasonically cleaned in acetone and subsequently in ethanol for 15 min, respectively, and then dried with pure nitrogen flow.

After being pumped down to a base pressure of 5×10^{-4} Pa, the deposition chamber was filled with high purity (99.999%) Ar and O_2 mixture gas. The O_2-Ar ratio was fixed as 1.0 : 49.0, 1.5 : 48.5, and 2.0 : 48.0, respectively (the unit is sccm). The total gas pressure was maintained at ~1.0 Pa. An rf power of 200 W was applied to the V target. During deposition, the substrate temperature was kept at 450°C for the better crystallinity of VO_2 thin films. To improve the film homogeneity, the substrates were rotated along the vertical axis at a speed of 10 rpm.

The structure of the films was characterized by Raman spectrometer (Renishaw inVia Raman microscope) using a 514.5 nm laser. The optical transmittance was measured at a photon energy range of 0.73–5.05 eV at 26°C and 95°C by a spectrophotometer (Hitachi Corp., Model UV-4100). Temperature was measured using a PT100 temperature sensor in contact with the films and was controlled via a temperature controlling unit. Heating was controlled through a temperature-controlling unit. Hysteresis loops were measured by collecting the transmittance of films at a fixed photon energy (0.83 eV) at a temperature interval of ~2.0°C. Spectroscopic ellipsometry (SE J. A. Woollam M-2000) measurements were carried out between photon energies of 0.73 and 5.05 eV at 75° angle of incidence and the results were modeled using a commercial software.

3. Results and Discussion

3.1. Structural Characterization. Raman measurements were conducted to examine the effect of O_2-Ar ratio on the microstructure of VO_2 (Figure 1(a)). The Raman spectrum at room temperature shows characteristic vibration modes for the M_1 semiconducting phase of VO_2. Comparing to previous works, Raman peaks are identified as 194(Ag), 223(Ag), 262(Bg), 307(Bg), 391(Ag), 492(Ag), and 618(Ag) cm^{-1} [9–11]. No Raman shifts for other kinds of vanadium oxides and any types of other polymorphs of VO_2 (M_2/T) [12, 13] were identified within the measurement accuracy (±0.2 cm^{-1}). The XRD spectra are shown in Figure 1(b). All peaks can be indexed to VO_2(M) and (011) was the prominent plane for VO_2 thin film. No reflections due to other VO_x phases such as V_4O_7, V_6O_{13} and V_3O_7 were observed [14, 15].

3.2. Optical Properties of the VO_2 Films. Figures 2(a) and 2(b) show the transmittance and absorptivity spectra of the prepared VO_2 thin films at different O_2-Ar ratios. The SMT transition is clearly observed with a dramatic change in the infrared transmittance with varied temperature ranges. The absorption edge, luminous (lum) transmittance (T_{lum}, 1.64–3.27 eV), and near-infrared (NIR) transmittance (0.73–1.64 eV) at the high temperature of 95°C were almost the same for all of the samples studied here. However, low temperature (below 26°C) phase $VO_2(M_1)$ showed a gradually decreased NIR transmittance but increased absorptivity with decreasing O_2-Ar ratios.

Thermooptical hysteresis curves were deduced by measuring the transmittance at 0.83 eV with varying temperatures, which are shown in Figure 2(c). For comparison, the vertical axis of this figure has been normalized as X. From the X-temperature (T) data, a plot of dX/dT was obtained, yielding one peak with a well-defined maximum.

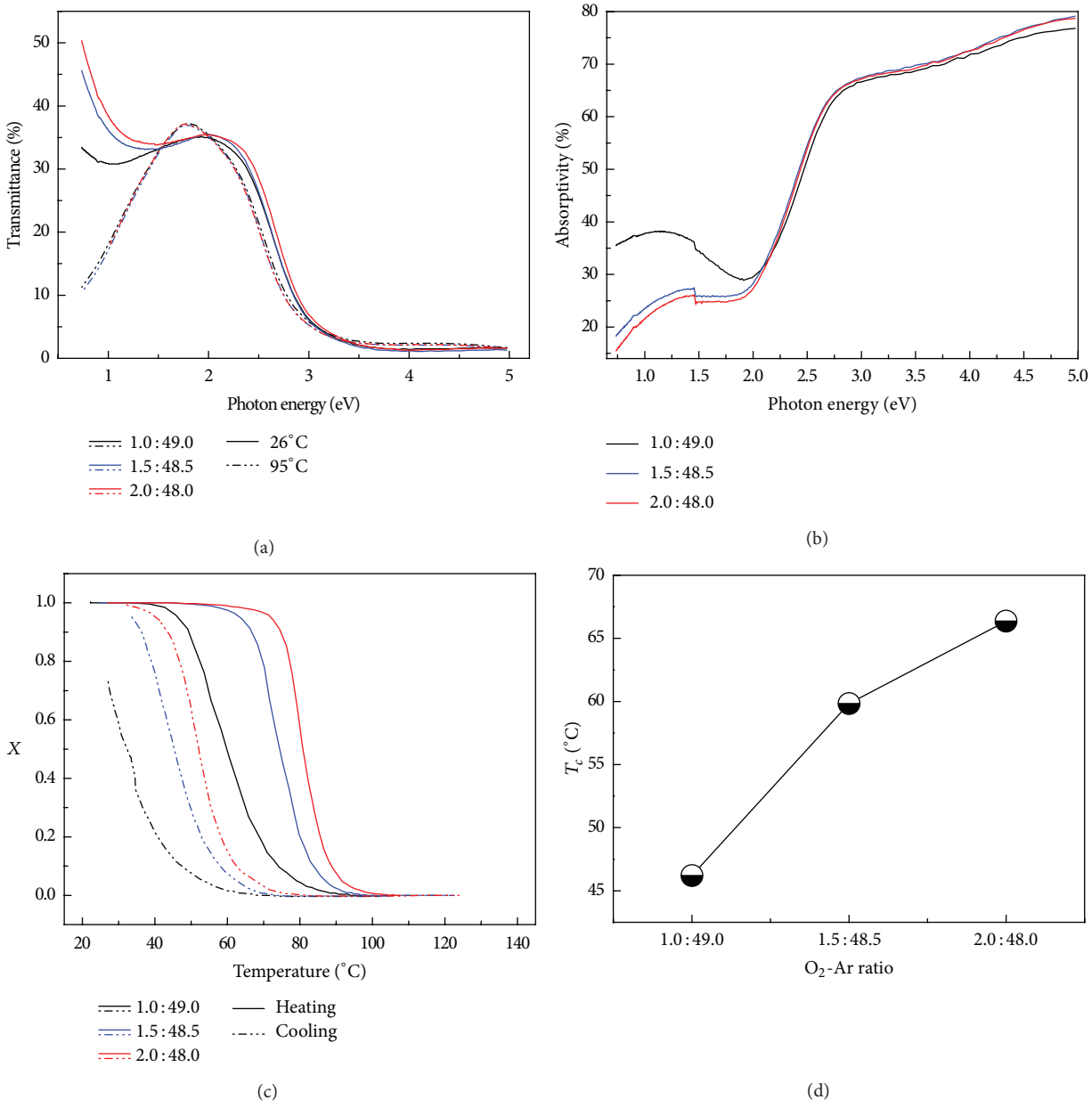

FIGURE 2: (a) Transmittance spectra of VO_2 films deposited at different O_2-Ar ratios. Solid and dashed lines refer to low temperature (26°C) and high temperature (95°C), respectively. (b) Low temperature (M_1 phase) absorptivity spectra. Thermal hysteresis loops of optical transmittance at photon energy of 0.83 eV and phase transition temperature T_c are shown in (c) and (d).

Each of the dX/dT curves has been analyzed with a Gaussian function using the single peak fitting module of Originpro 8.0 software. The temperature corresponding to the maximum of dX/dT was defined as the phase transition temperature during a heating/cooling cycle; T_1 and T_2 represent the SMT temperature of heating and cooling branches, respectively. The SMT temperature was defined as $T_c = (T_1 + T_2)/2$. As shown in Figure 2(d), the SMT temperatures were 46.2°C, 59.8°C, and 66.4°C for VO_2 films deposited at the O_2-Ar ratio of 1.0 : 49.0, 1.5 : 48.5, and 2.0 : 48.0, respectively. The phase transition temperature T_c consistently decreased as the O_2-Ar ratio decreased. It was pointed out that vanadium interstitials and/or oxygen vacancies could reduce the SMT temperature of VO_2 [16], which is also responsible for the decreased SMT temperatures at low O_2-Ar ratios of this work. Low O_2-Ar ratios can introduce both extra electrons and internal strains in nonstoichiometric VO_2 (related data was revealed in a paper submitted to Thin Solid Films, Manuscript Number: TSF-D-13-00641).

3.3. Optical Constant. The electronic transitions, optical constants, and optical band gap (OBG) in the vicinity of the phase transition temperature have been investigated by Li et al. [17]. For a standard bulk VO_2 sample, when

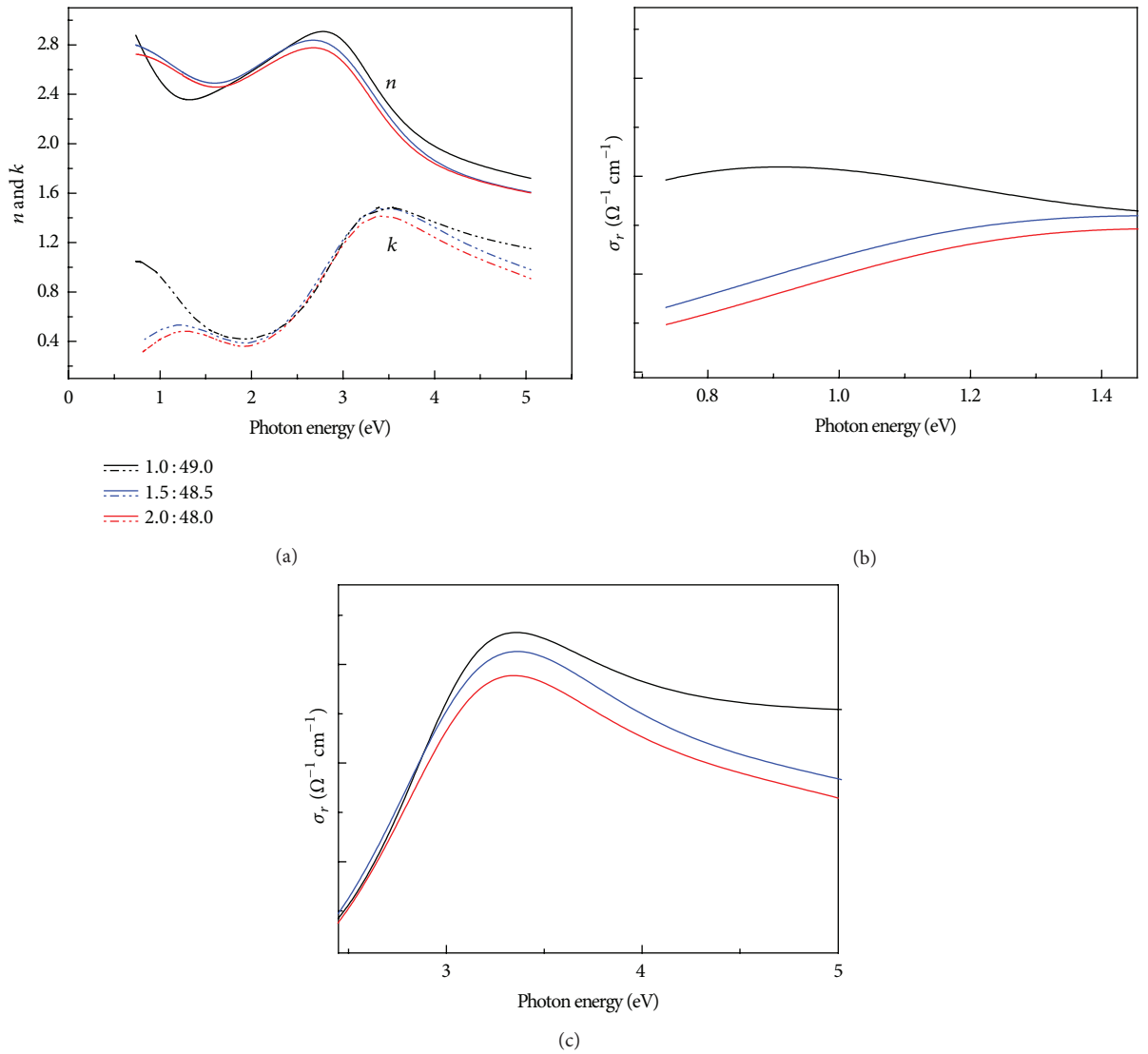

FIGURE 3: Refractive index n, extinction coefficient k, and optical conductivity σ_r of low temperature phase VO_2 deposited at different O_2-Ar ratios.

temperature was increased to 67°C, contributions from the Drude response become more prominent. The extinction coefficient k and the optical conductivity σ_r values at the NIR region rapidly increase with increasing temperature. In this research, electron concentration increases with decreasing O_2-Ar ratios and the Drude response is also responsible for the increased k and σ_r value at the NIR region (Figure 3). However, refractive index n was not significantly changed.

3.4. Band Gap. The indirect OBG can be estimated using the power law:

$$(\alpha E)^{1/2} \propto \left(E - E_g\right), \tag{1}$$

where $\alpha = 4\pi k/\lambda$ is the absorption coefficient and E_g is the OBG energy. The E_g value is extrapolated by the linear portion of the plot to $(\alpha E)^{1/2} = 0$.

Two electronic transitions can be uniquely assigned, as shown in Figures 4(a) and 4(b). The gaps correlated with absorption edge (E_1) at varied O_2-Ar ratios are almost the same (~2.0 eV); consequently, the absorption edge was not significantly changed, as shown in Figure 2(a). However, the optical band gap corresponding to SMT (E_2) decreases from 0.53 to 0.18 eV with decreasing O_2-Ar ratios, as shown in Figures 4(b) and 4(d). The OBG E_2 of semiconducting VO_2 can be assigned to the indirect transition from the top of filled $d_{//}$ bands to the bottom of empty π^* band, as shown using a red arrow in Figure 4(c). Note that E_2 at an O_2-Ar ratio of 2.0 : 48.0 is similar to that from a previous report by theoretical calculation (0.6 eV) [18] and experimental results by photoemission spectroscopy (0.6 eV) [2]. Besides, the 0.41 eV band gap of the VO_2 film prepared at an O_2-Ar ratio of 1.5 : 48.5 agrees to a calculated intermediate structure at 339.8 K (0.36 eV) [18]. E_2 at 1.0 : 49.0 O_2-Ar ratio further decreased to 0.18 eV.

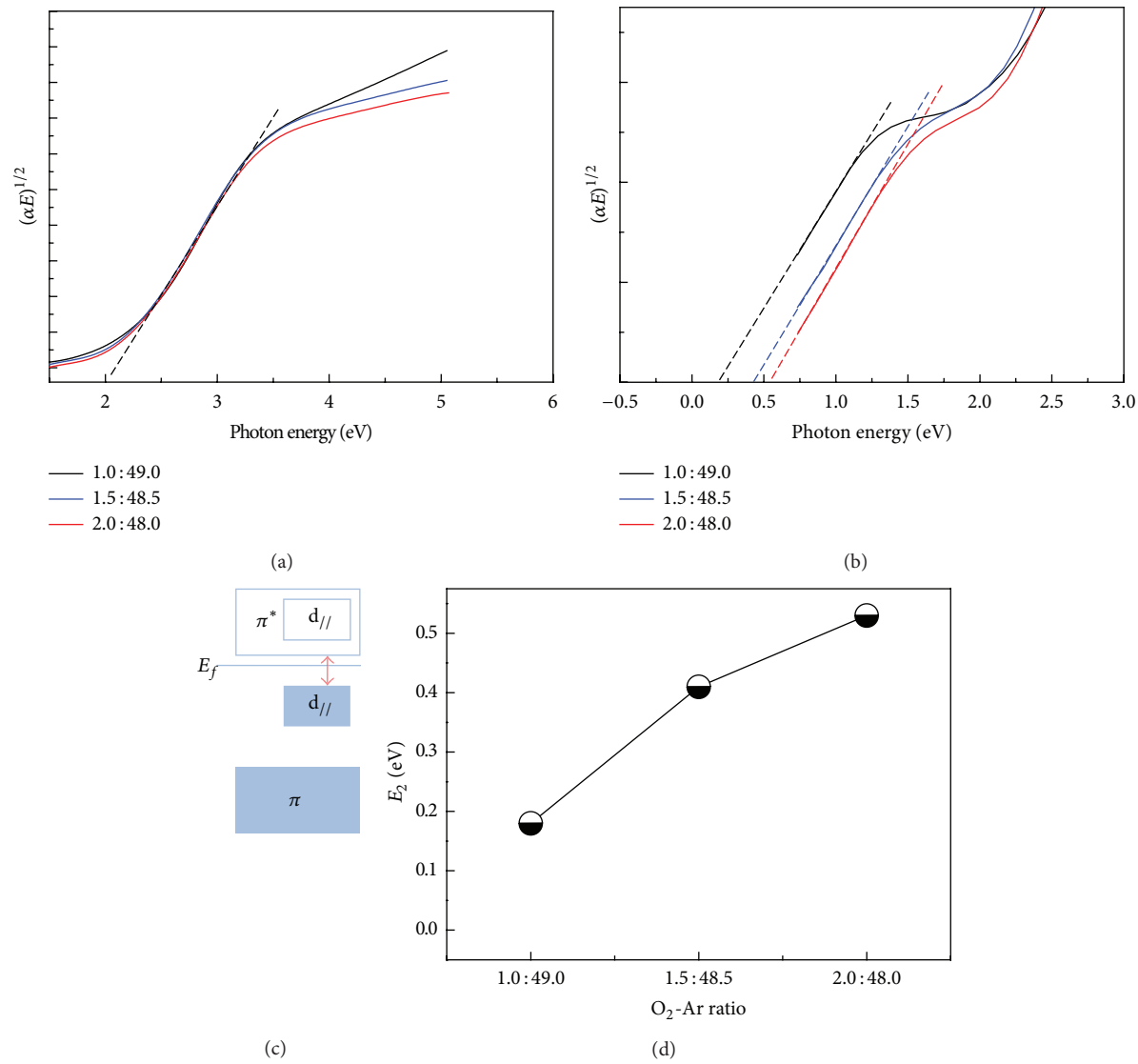

FIGURE 4: (a) and (b) $(\alpha E)^{1/2}$ versus E which is determined from extinction coefficient k and the extrapolating dashed lines are drawn to obtain the value of the band gap E_1 and E_2, respectively. (b) is the enlarged low photon energy portion of $(\alpha E)^{1/2}$ versus E. (c) Schematic diagram of electronic band structures in the VO_2 film. (d) Variation of optical band gap E_2 of VO_2 thin films deposited at different O_2-Ar ratios.

When decreasing O_2-Ar ratios, the filled $d_{//}$ bands and the empty π^* band are shifted to the higher and lower energy, respectively. Both the $d_{//}$ and π^* bands gradually moved closely, resulting in a redshift of E_2. The decreasing E_2 results in a decrement in the SMT energies; therefore the SMT temperature decreased with decreasing O_2-Ar ratios. Moreover, with decreasing the O_2-Ar ratio, the NIR transmittance of the film evidently decreases. This behavior is because the bandgap E_2 of the film, which is narrowing at low O_2-Ar ratios, is different at the distinct O_2-Ar ratio regions. It can enhance the electronic transitions and results in more interband absorptions at lower O_2-Ar ratios, as shown in Figure 2(b).

4. Conclusions

To summarize, diverse phase transformation properties are reported for phase pure $VO_2(M_1)$ thin films grown at different oxygen partial pressures by reactive magnetron sputtering. The transmittance and absorptivity spectra below phase transition temperatures are closely related to O_2-Ar ratios. The phase transition temperature T_c decreased from 66.4°C to 46.2°C as the O_2-Ar ratio decreased from 2.0 : 48.0 to 1.0 : 49.0. The optical constants of the $VO_2(M_1)$ thin films have been determined between 0.73 and 5.05 eV. The near-infrared extinction coefficient k and optical conductivity σ_r increase with decreasing O_2-Ar ratios. Moreover,

two electronic transitions were identified. The energy gaps correlated with absorption edge at varied O_2-Ar ratios are almost the same, while the optical band gap corresponding to semiconductor-to-metal phase transition decreases from 0.53 to 0.18 eV with decreasing O_2-Ar ratios.

Conflict of Interests

The authors declare that there is no conflict of interests regarding the publication of the article.

Acknowledgments

This study was financially supported by the National Natural Science Foundation of China (NSFC, no. 51032008, 51272273, 51102270, 51272271, 51172265, and 51372264), the high-tech project of MOST (2012AA030605 and 2012BAA10B03), and Science and Technology Committee of Shanghai (no. 13PJ1409000).

References

[1] F. J. Morin, "Oxides which show a metal-to-insulator transition at the neel temperature," *Physical Review Letters*, vol. 3, no. 1, pp. 34–36, 1959.

[2] T. C. Koethe, Z. Hu, M. W. Haverkort et al., "Transfer of spectral weight and symmetry across the metal-insulator transition in VO_2 ," *Physical Review Letters*, vol. 97, no. 11, Article ID 116402, 2006.

[3] Z. Zhang, Y. Gao, H. Luo et al., "Solution-based fabrication of vanadium dioxide on F:SnO_2 substrates with largely enhanced thermochromism and low-emissivity for energy-saving applications," *Energy and Environmental Science*, vol. 4, no. 10, pp. 4290–4297, 2011.

[4] Y. F. Gao, S. B. Wang, L. T. Kang et al., "VO_2-Sb:SnO_2 composite thermochromic smart glass foil," *Energy and Environmental Science*, vol. 5, pp. 8234–8237, 2012.

[5] Y. Gao, H. Luo, Z. Zhang et al., "Nanoceramic VO_2 thermochromic smart glass: a review on progress in solution processing," *Nano Energy*, vol. 1, no. 2, pp. 221–246, 2012.

[6] P. P. Boriskov, A. A. Velichko, A. L. Pergament, G. B. Stefanovich, and D. G. Stefanovich, "The effect of electric field on metal-insulator phase transition in vanadium dioxide," *Technical Physics Letters*, vol. 28, no. 5, pp. 406–408, 2002.

[7] C. H. Griffiths and H. K. Eastwood, "Influence of stoichiometry on the metal-semiconductor transition in vanadium dioxide," *Journal of Applied Physics*, vol. 45, no. 5, pp. 2201–2206, 1974.

[8] J. Li and J. Dho, "Anomalous optical switching and thermal hysteresis behaviors of VO_2 films on glass substrate," *Applied Physics Letters*, vol. 99, no. 23, Article ID 231909, 2011.

[9] A. C. Jones, S. Berweger, J. Wei, D. Cobden, and M. B. Raschke, "Nano-optical investigations of the metal-insulator phase behavior of individual VO_2 microcrystals," *Nano Letters*, vol. 10, no. 5, pp. 1574–1581, 2010.

[10] P. Schilbe, "Raman scattering in VO_2 ," *Physica B*, vol. 316-317, pp. 600–602, 2002.

[11] J. Y. Chou, J. L. Lensch-Falk, E. R. Hemesath, and L. J. Lauhon, "Vanadium oxide nanowire phase and orientation analyzed by Raman spectroscopy," *Journal of Applied Physics*, vol. 105, no. 3, Article ID 034310, 2009.

[12] C. Marini, E. Arcangeletti, D. di Castro et al., "Optical properties of $V_{1-x}Cr_xO_2$ compounds under high pressure," *Physical Review B*, vol. 77, no. 23, Article ID 235111, 2008.

[13] J. M. Atkin, S. Berweger, E. K. Chavez et al., "Strain and temperature dependence of the insulating phases of VO_2 near the metal-insulator transition," *Physical Review B*, vol. 85, no. 2, Article ID 020101, 2012.

[14] Y. D. Ji, T. S. Pan, Z. Bi et al., "Epitaxial growth and metal-insulator transition of vanadium oxide thin films with controllable phases," *Applied Physics Letters*, vol. 101, Article ID 071902, 2012.

[15] P. Jin and S. Tanemura, "Formation and thermochromism of VO_2 films deposited by RF magnetron sputtering at low substrate temperature," *Japanese Journal of Applied Physics*, vol. 33, no. 3 A, pp. 1478–1483, 1994.

[16] S. Zhang, I. S. Kim, and L. J. Lauhon, "Stoichiometry engineering of monoclinic to rutile phase transition in suspended single crystalline vanadium dioxide nanobeams," *Nano Letters*, vol. 11, no. 4, pp. 1443–1447, 2011.

[17] W. W. Li, Q. Yu, J. R. Liang et al., "Intrinsic evolutions of optical functions, band gap, and higher-energy electronic transitions in VO_2 film near the metal-insulator transition region," *Applied Physics Letters*, vol. 99, no. 24, Article ID 241903, 2011.

[18] T. Yao, X. Zhang, Z. Sun et al., "Understanding the nature of the kinetic process in a VO_2 metal-insulator transition," *Physical Review Letters*, vol. 105, no. 22, Article ID 226405, 2010.